Mycologia Iranica 11(2): 41– 49, 2024 Original Article DOI:10.22043/MI.2024.367956.1297

Identification and characterization of *Neodidymelliopsis cynanchi*, the causal agent of milkweed leaf lesions

A. Habibi ✉
Department of Biodiversity, Institute of Science and High Technology and Environmental Sciences, Graduate University of Advanced Technology, Kerman, Iran

R. Mostowfizadeh-Ghalamfarsa
Department of Plant Protection, School of Agriculture, Shiraz University, Shiraz, Iran

Abstract: *Calotropis procera* is a shrub or small tree growing in tropical regions of the southern provinces of Iran. The economic benefits of the shrub include the use of latex and extract in traditional medicine. In a survey conducted in the southern provinces of Iran, leaf lesion symptoms were observed on *C. procera* shrubs. The purpose of the current study was to identify and characterize putative pathogens causing these symptoms. Isolations from the symptomatic tissues yielded predominantly a fungus belonging to the *Didymellaceae* family of *Ascomycota*. The causal agent was identified as *Neodidymelliopsis cynanchi*, based on morphological characteristics, and multilocus phylogenetic analysis using ITS, LSU, *rpb2,* and *tub2* sequences. Pathogenicity tests on four-month-old seedlings of *C. procera* revealed that the isolates caused typical leaf lesions on the host. To the best of our knowledge, this is the first report of *N. cynanchi* causing disease on *C. procera* worldwide and the first report of the occurrence of this species in Iran.

Keywords: *Calotropis procera*, *Didymellaceae*, Morphology, Pathogenicity, Phylogenetic analysis.

INTRODUCTION

Calotropis procera (Aiton) W.T.Aiton, also known as milkweed (Stabragh in Persian), belongs to *Apocynaceae* family (Wilkinson 2005). This plant species is native to Asia and Africa (Ghasemi et al. 2012) and has been introduced into Australia, central and southern America, the West Indies, and the Mascarene Islands (Rahman & Wilcock 1991). This shrub mainly grows in tropical regions of southern Iran. It is a drought-resistant and salt-tolerant species, growing along roadsides, watercourses, river flats, and coastal dunes, and is often prevalent in disturbed areas (Hassan et al. 2015). *Calotropis procera* has significant socioeconomic value and is used extensively in traditional medicine systems for the treatment of colds, fever, skin diseases, hair loss, asthma, rheumatism, eczema, indigestion, and diarrhea (Ahmad Nejhad et al. 2023, Al-Rowaily et al. 2020). Additionally, this plant species also is used for the control of soil pollution and soil erosion (Farrar et al. 2020).

A few fungi have been reported to occur on *C. procera* in Iran. According to Ershad (2022), the following fungi have been reported from this plant species: *Passalora calotropidis* (Ellis & Everh.) U. Braun, *Ascochyta calotropidis* Sacc., and *Alternaria* sp. Globally, the fungi isolated from *C. procera* include *Ascochyta tripolitana* Sacc. & Trotter from Libya; *Cladosporium calotropidis* F. L. Stevens from Puerto Rico, *Coniothyrium calotropidis* S. Ahmad, *Diplodia calotropidis* S. Ahmad and *Hendersonia calotropidis* S. Ahmad from Pakistan; *Gloeosporium* (= *Colletotrichum*) *calotropidis* El. & Ev. and *Napicladium calotropies* H. Morstatt, From East Africa; *Phoma calotropidis* (Thum.) Sacco from Sudan and Senegal; *Passalora calotropidis* and *Puccinia obliqua* Berk. & M.A. Curtis from Australia (Barreto et al. 1999, Wilkinson 2005).

During surveys conducted from 2020 to 2022, lesions on leaves and twigs of *C. procera* were noticed in Hormozgan, and Kerman Provinces, Iran. The objectives of this study were to identify, characterize, and test the pathogenicity of the causal agent of the observed symptoms on *C. procera* using morphological features and phylogenetic analysis of DNA sequence data.

MATERIALS AND METHODS

Sampling and fungal isolation

Symptomatic leaves of milkweed (*C. procera*) were collected in January 2020 and February 2021 from Tezerj, Hormozgan Province, and in February 2022 from Orzueeyeh, Kerman Province, Iran. The interfaces between healthy and infected tissue were cut into small pieces. The leaf pieces were surface-disinfected with 1% sodium hypochlorite for 2 min, 1 min in 70 % ethanol, and then rinsed twice in sterile distilled water. The surface-sterilized leaf fragments

Submitted 10 Dec. 2024, accepted for publication 16 Dec. 2024
✉ Corresponding Author: E-mail: a.habibi@kgut.ac.ir

https://mij.areeo.ac.ir

were placed on potato dextrose agar (PDA; 1 L extract of 300 g boiled potato, 20 g glucose, 16 g agar). Plates were incubated at 25 °C in the dark for 7 days. Single-spored isolates were obtained following the protocol of Choi et al. (1999) and transferred to fresh PDA plates. For long-term storage, the isolates were cultured on PDA plates containing sterilized filter paper pieces. The filter papers were dried and stored at -20 °C (Peever et al. 1999).

Morphological characteristics

Pure isolates obtained from the infected leaf tissues were grown on oatmeal agar (OA; 30 g oatmeal, 16 g agar, 1 L distilled water), malt extract agar (MEA; 20 g malt extract, 15 g. agar, 1 L distilled water), and PDA (recipes according to Crous et al. 2009). Petri plates were incubated at 25 °C under 12 h of light and 12 h of darkness for a period of three weeks. The morphological characteristics and microscopic structures, including the morphology of conidiomata, the shape and type of conidiogenous cells and conidia, the number of ostioles, and the thickness of the pycnidial wall, were examined using a light microscope (Leica Microsystems, Germany). Images were acquired using a Dino-eye Eyepiece USB camera (Dino-Lite, Torrance, CA, USA). At least 30 measurements were made for the microscopic structures. Growth rates of three isolates (ME0, ME1, ME2) were estimated at 6 temperatures (4, 10, 15, 20, 25, and 30 °C) on PDA in the dark. Colony diameters were measured as the average of two perpendicular transects per colony after 3, 7, and 14 days of growth in mm.

DNA extraction, PCR amplification and sequencing

Mycelia were scraped from the surface of actively growing colonies on PDA after one week and crushed using liquid nitrogen. The cells were lysed using a CTAB solution (Doyle and Doyle 1987), and the DNA extraction was performed using the DNG™-Plus extraction kit (CinnaGen, Tehran, Iran), according to the manufacturer's instructions. Four loci were amplified: the nuclear ribosomal internal transcribed spacer (ITS) of rDNA, the partial beta-tubulin gene (*tub2*), the partial large subunit nrRNA gene (28S nrDNA; LSU) and the RNA polymerase second largest subunit (*rpb2*) gene. These loci were amplified using the primer pairs ITS1/ITS4 (White et al. 1990), Bt2a/Bt2b (Glass & Donaldson 1995), LR0R/LR5 (Vilgalys & Hester 1990, Rehner and Samuels 1994), and RPB2-5F2/RPB2-7cR (Liu et al. 1999, Sung et al. 2007), respectively. PCR mixtures were prepared in 25 µL total reaction volumes containing 0.5 µL template DNA, 0.5 µL (10 pM) each primer, 12.5 µL *Taq* DNA polymerase 2 × Master Mix RED (Ampliqon, Denmark), and 11 µL deionized distilled water. Amplifications were performed in a Biometra TAdvanced Thermal Cycler (Biometra, Göttingen, Germany). PCR conditions for LSU, ITS and *tub2* were an initial denaturation step of 5 min at 94 °C, followed by 35 cycles of denaturation at 94°C for 30 s, annealing at 58 °C (ITS), 55 (*tub2*) and 56°C (LSU) for 30 s and extension at 72°C for 30 s; and a final elongation step of 7 min at 72 °C (Chen et al. 2015). The PCR conditions for *rpb2* were an initial denaturation at 94 °C for 5 min, followed by 35 cycles of denaturation at 95 °C for 45 s, annealing at 56 °C for 80 s, and extension at 72 °C for 2 min, with a final extension step at 72 °C for 10 min (Hou et al. 2020). The PCR product sequencing was performed by Pishgam (Pishgam Biotech Co., Tehran, Iran). Novel sequences generated in this study were deposited in GenBank (http://www.ncbi.nlm.nih.gov/genbank).

Table 1. The list of *Neodidymelliopsis cynanchi* isolates recovered from infected *Calotropis procera* shrubs in Hormozgan and Kerman Provinces, Iran and the generated sequences in this study.

Isolate	Collection date	Geographic location	Source	GenBank Accession Numbers			
				RPB2	Tub2	ITS	LSU
ME0	10-Jan-2020	Tezerj, Hormozgan	leaf	PQ653985	PQ653990	PQ637462	PQ637467
ME1	10-Jan-2020	Tezerj, Hormozgan	leaf	PQ653986	PQ653991	PQ637463	PQ637468
ME2	25-Jan-2021	Tezerj, Hormozgan	leaf	PQ653987	PQ653992	PQ637464	PQ637469
ME4-1	25-Feb-2021	Orzueeyeh, Kerman	leaf	PQ653988	PQ653993	PQ637465	PQ637470
ME5-1	25-Feb-2021	Orzueeyeh, Kerman	leaf	PQ653989	PQ653994	PQ637466	PQ637471

Phylogenetic analyses

The quality of the obtained sequences was checked and manually edited using Geneious software (Biomatters Inc., USA) where necessary. Homology searches for the initial species identification were performed using the Basic Local Alignment Search Tool (BLASTn algorithm) (https://blast.ncbi.nlm.nih.gov/Blast.cgi) against sequences in GenBank database. To determine the taxonomic status of the obtained isolates in comparison to related species a phylogenetic analysis was conducted using a combined data set of all sequenced markers (ITS, LSU, *tub2*, *rpb2*) together

with the sequences of reference taxa from GenBank (Supplementary Table). Sequences were aligned using ClustalW (Thompson et al. 2002). Phylogenetic analyses were performed using the Bayesian inference (BI) method. The most appropriate nucleotide substitution models for each data set were determined for each data set with jModelTest (version 2.1.4) (Posada 2008) using the Bayesian information criterion (BIC). Analyses were conducted using MrBayes v. 3.2.2 (Ronquist et al. 2012). Four Markov chains were run for 10 million generations, with a burn-in fraction set to 0.25 and the remaining trees were used to calculate the posterior probabilities in the consensus tree. The resulting phylogenetic tree was visualized using FigTree v. 1.4.0 (Rambaut 2012). *Xenodidymella applanata* (Niessl) Qian Chen & L. Cai (CBS115578) was used as an outgroup to root phylogenetic trees.

Fig 1. Symptoms on various parts of milkweed (*Calotropis procera*) infected by *Neodidymelliopsis cynanchi*. a: A defoliated shrub; b–d: Reddish-brown necrotic lesions with central beige and yellow halos on leaves; e: Elongated brown lesion on a petiole; f: Elongated lesion on a twig.

Pathogenicity tests

Koch's postulates were performed on four-month-old potted seedlings of *C. procera* (local cultivar) obtained from local nurseries in Rudan County, Hormozgan, Iran. Strain ME1 was used for the pathogenicity test on ten seedlings. For inoculum production, conidia were harvested by adding 10 mL of sterile distilled water to 30-day-old colonies grown on PDA, gently scraping with a glass rod, and then filtering through a cheesecloth. Conidial suspensions were adjusted to 1×10^6 conidia/ml with a hemocytometer and applied to the entire plant until runoff occurred with a hand sprayer. Control plants were sprayed with sterile water. Inoculated plants were kept in a humid chamber at 20 °C for five days to maintain high relative humidity and then transferred to outdoors. Seedlings were visually inspected for symptoms following inoculations. When the leaf spots began to appear, the fungal species were re-isolated from the margins of the leaf spots onto PDA, and identification of the pathogen was performed using morphological characteristics.

RESULTS

Disease symptoms, and fungal isolates from *C. procera*

During 2020-2021, reddish-brown necrotic lesions were observed on milkweed (*C. procera*) leaves in Tezerj, Hormozgan Province, and Orzueeyeh, Kerman Province, Iran. The initial symptoms were red-brown spots appearing on leaves, which later expanded to larger, irregular lesions with a yellow halo surrounding them. In the developed lesions, the center area became beige,

with concentric zones of embedded black pycnidia on both sides of the lesion. Similar elongated lesions were also observed on twigs and petioles (Fig 1). Defoliation was observed in some shrubs. A collection of 12 isolates was obtained from lesions of the diseased leaves (Table 1).

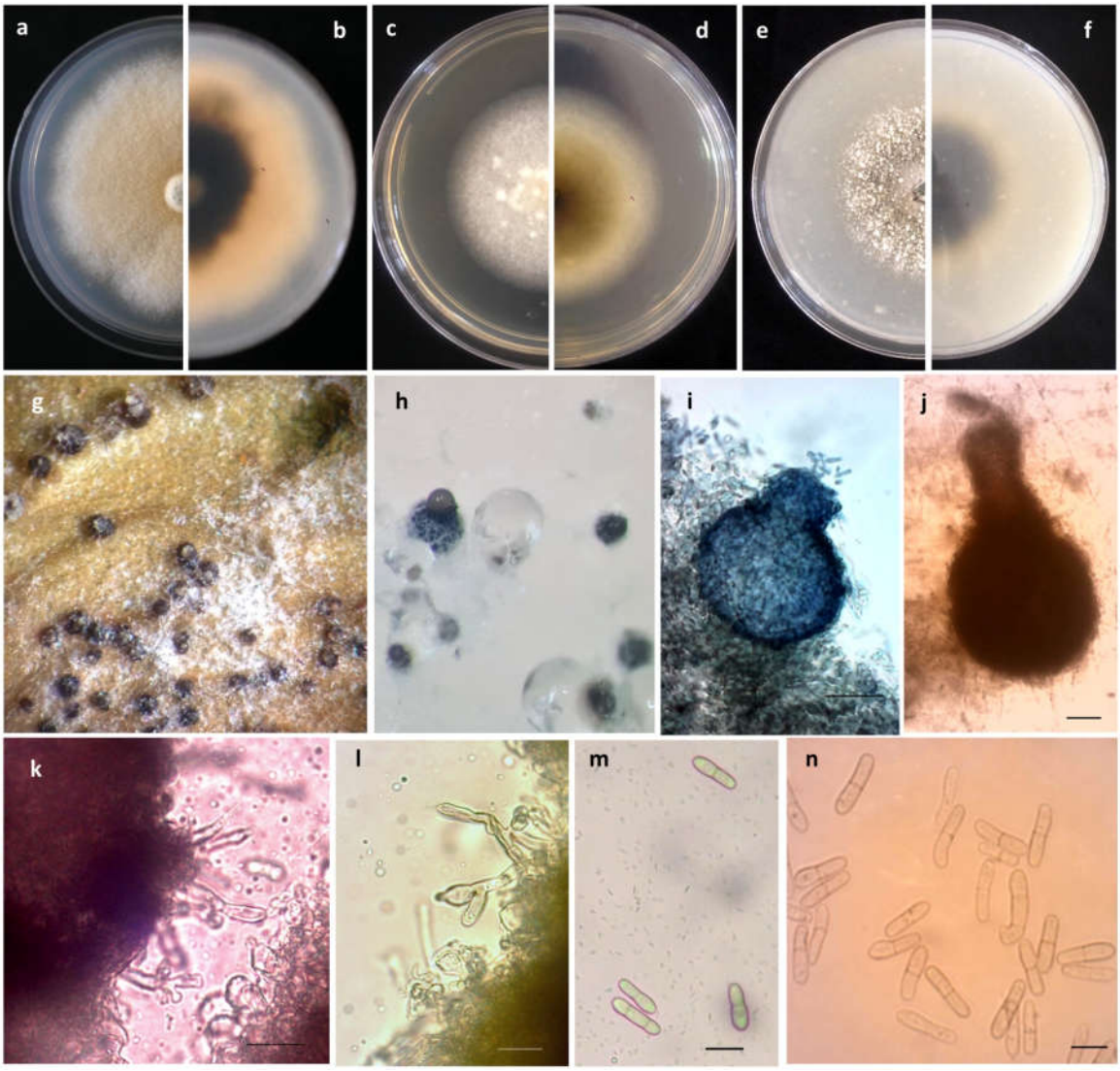

Fig 2. Morphological characters of *Neodidymelliopsis cynanchi*. a–f: Colony on PDA, MEA, and OA, front (left) and reverse (right) views after 10 days at 25 °C; g: Pycnidia forming on host leaf; h: Pycnidia forming on PDA; i: A longitudinal section of a pycnidium. j: Pycnidium; k–l: Conidiogenous cells; m–n: Conidia. Scale bars: i–j= 50 µm, k–l= 20 µm, m–n= 10 µm.

Morphological observations

The colonies on PDA were white to creamy; the reverse was buff at the margins, and dark brown at the center; on MEA they were white; the reverse was brown to yellowish brown, creamy near the margins; and on OA they were white to cream, with the reverse being pale brown near the margins, dark brown to black at center (Fig 2. a–f). The optimum growth temperature on PDA was 20 °C. The mycelial radial growth rate on PDA (mean value mm/day) was 3.3 ±0.2 mm/d at 20 °C among five isolates. Conidiomata were pycnidial, ellipsoidal to subglobose, and ostiolate, 225–380 × 160–230 µm (n= 30; av. 310 ±64 × 197.5 ±28 µm). The ostiole was single and papillate in young pycnidia while developing into elongated necks (Fig 2. g–j). Conidiogenous cells were phialidic, hyaline, smooth, ampulliform to doliform, 4.5–10.3 × 7.5–17.8 µm (Fig 2. k–l). Conidia were oblong to

cylindrical, smooth, thin-walled, hyaline, 1–2 septate, 14.8–18.2 × 3.2–4.9 µm (n= 30; av. 16.9 ±2.1 × 3.9 ±0.4 µm) (Fig 2. m–n).

Molecular identification

Obtained sequences were submitted to GenBank under the accession numbers PQ637467-PQ637471 for LSU, PQ637462-PQ637466 for ITS, PQ653990-PQ653994 for *tub2*, and PQ653985-PQ653989 for *rpb2* (Table 1). The BLAST search showed that our isolates had the closest match to the *Neodidymelliopsis* species. The concatenated alignment of ITS, LSU, *rpb2,* and *tub2* sequences consisted of 25 taxa, including representatives of species in the *Neodidymelliopsis* genus. The alignment contained 2,387 characters. The GTR +G model was selected as optimal for ITS, LSU, *rpb2,* and *tub2* based on the result of the jModeltest. In the phylogenetic tree, the sequence of our isolates clustered in the same clade with *Neodidymelliopsis cynanchi* (Fig 3).

Pathogenicity

The ME1 isolate was selected to confirm Koch's postulate on four-month-old potted seedlings of *C. procera*. The inoculated seedlings developed reddish-brown necrotic lesions starting three weeks post-inoculation (Fig. 4). The observed lesions were similar to those observed in the field. No symptoms were observed in the control plants. The fungus that was re-isolated from leaf lesions had the same morphology and colony coloration as the fungus in the inoculum.

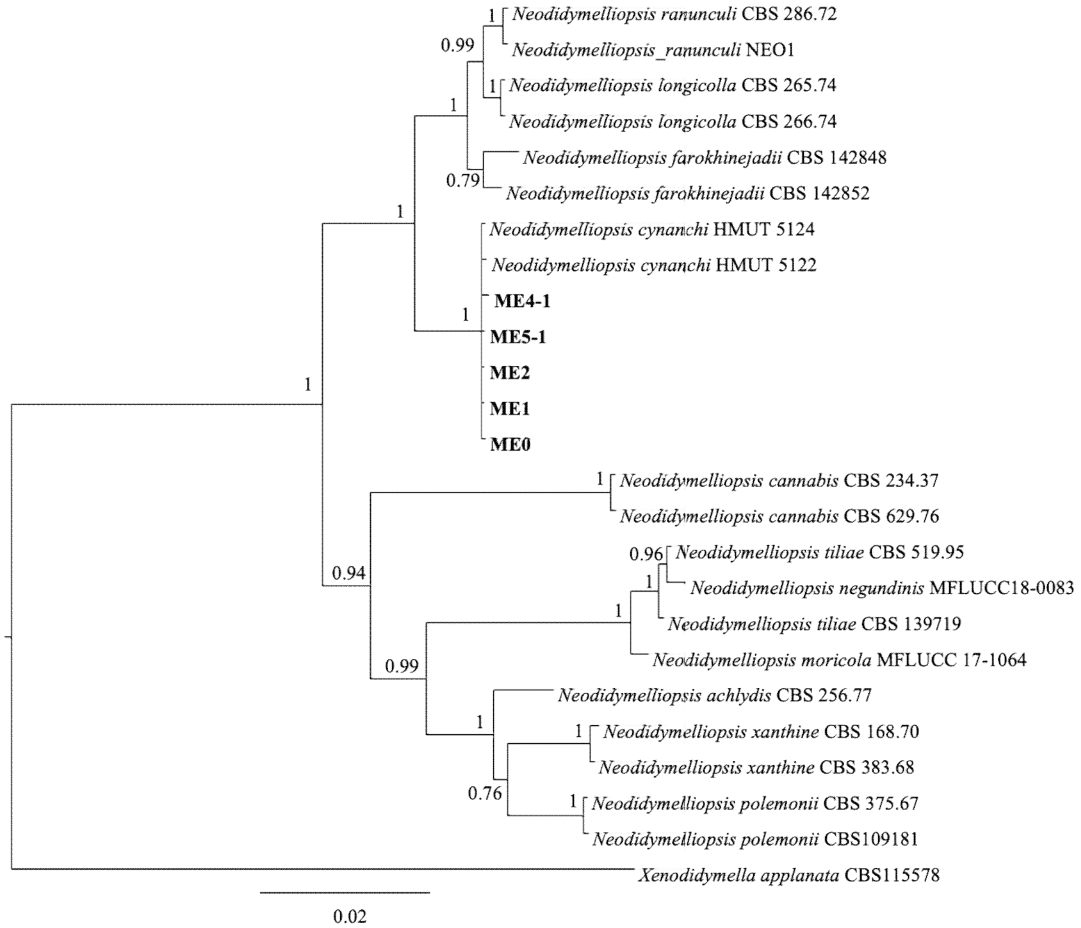

Fig 3. Phylogenetic tree based on analysis of the combined sequences of ITS, LSU, *rpb2*, and *tub2* from recovered isolates of *Neodidymelliopsis* spp. and related species using the Bayesian method. The scale bar represents substitutions per site. The tree was rooted using *Xenodidymella applanata* (CBS115578). Numbers on the branches are posterior probabilities.

Fig 4. Results of pathogenicity tests of *Neodidymelliopsis cynanchi* on milkweed seedlings. Infected seedling (right); control seedling (left).

DISCUSSION

The objective of this research was to determine the causal agent of leaf lesions observed on milkweed (*C. procera*). Based on the combined results of morphological characteristics, multilocus phylogenetic analysis using ITS, LSU, *rpb2,* and *tub2* sequences, and pathogenicity tests, the pathogen was identified as *Neodidymelliopsis cynanchi* B. Xu & J.G. Song. To our best knowledge, this ascomycete species has not previously been reported as a pathogen of milkweed. This is the first report of *N. cynanchi* occurring in Iran.

The morphological characteristics of the isolates obtained in this study were consistent with those described by Qian et al. (2024) for *N. cynanchi*. However, due to different environmental conditions, there are slight differences between our isolates and *N. cynanchi* description. Our isolates were morphologically similar to *N. cynanchi* in conidial shape but differed in producing smaller conidia (16.9 × 3.9 vs. 21 × 6 µm) and longer conidiogenous cells (7.5–17.83 × 4.43–10.34 vs. 6–10 × 5–10 µm) (Qian et al. 2024). Morphological characteristics are relatively conserved in *Phoma*-like taxa, including features such as the shape and dimensions of pycnidia, conidiogenous cells, and conidia (Chen et al. 2015). Chen et al. (2015) studied the genera in the *Ascochyta-Didymella-Phoma* complex and stated that many of the species clustered in different phylogenetic lineages shared overlapping morphological features. Therefore, morphological features may not provide sufficient distinctions to differentiate most of the genera in *Didymellaceae*. They concluded that reliable identification in *Didymellaceae* should be based on DNA sequence data combined with morphology and ecology.

Combined sequences of ITS, LSU, *tub2*, and *rpb2* regions have been successfully used to distinguish *Neodidymelliopsis* species (Chen et al. 2015, Chen et al. 2017, Ahmadpour et al. 2017, Qian et al. 2024). In the molecular phylogeny derived from the combined regions of ITS, LSU, *tub2,* and *rpb2* isolates from the present study clustered with *N. cynanchi* reported from leaf spot of *Cynanchum sibiricum* Willdenow in China (Qian et al. 2024). This highlights the effectiveness of using combined molecular data for accurate species identification in *Neodidymelliopsis* and underscores the importance of investigating phylogenetic relationships in understanding pathogen diversity.

Due to the unavailability of sequence data for some *Neodidymelliopsis* species, including *N. camporesii* D. Pem, Doilom & K.D. Hyde, *N. urticae* Manawas., Camporesi & K.D. Hyde, *N. salviae* Brahamanage, Camporesi & K.D. Hyde, and *N. tinkyukuku* E.C. Keirnan, M.H. Laurence, R.G. Shivas & Y.P. Tan, we were unable to include them in our multilocus phylogenetic analysis. Since *N. urticae* only has sequences for the ITS, LSU, and *rpb2* regions, *N.*

tinkyukuku has sequences only for its ITS and *rpb2* regions, *N. salviae* has data only for the ITS and LSU regions, and *N. camporesii* only has sequences for the ITS, LSU, and *tub2* regions, we could not conduct a comparative analysis of the four regions for these taxa. This limitation highlights the need for further genomic studies on these *Neodidymelliopsis* species to enable comprehensive phylogenetic analyses and enhance our understanding of their evolutionary relationships with our isolates.

The family *Didymellaceae* was established to accommodate the majority of species in *Phoma s. lat.* and related genera by de Gruyter et al. (2009), based on its type genus, *Didymella* Sacc. The *Didymellaceae* has undergone extensive revision based on phylogenetic analyses (Aveskamp et al. 2010, Chen et al. 2015). Chen et al. (2015) proposed nine genera (*Allophoma*, *Calophoma*, *Heterophoma*, *Neoascochyta*, *Neodidymelliopsis*, *Nothophoma*, *Paraboeremia*, *Phomatodes* and *Xenodidymella*) in *Didymellaceae*. *Neodidymelliopsis farokhinejadii* S.A. Ahmadp. & M. Mehrabi and *N. longicolla* L.W. Hou, Crous & L. Cai have been reported previously from Iran. *Neodidymelliopsis farokhinejadii* was isolated from dead branches of *Citrus* spp., *Conocarpus erectus* L., *Cupressus* sp., *Eucalyptus* sp., *Juglans regia* L. and *Ziziphus* sp. in southwestern Iran (Ahmadpour et al. 2017). *Neodidymelliopsis longicolla* has also been reported to cause lesion blight on *Papaver dubium* L. (*Papaveraceae*) (Razaghi and Zafari 2018) and dieback in citrus orchards (Soleimani et al. 2018) in Iran. The majority of members in *Didymellaceae* are plant-associated fungi (Chen et al. 2017) and only a few species were reported from other substrates (Aveskamp 2008). The present study further indicates that a large number of unknown *Didymellaceae* species exist in nature, especially from previously overlooked ecosystems, which should be prioritized for future research to better understand their diversity, ecological roles, and potential applications.

Artificial inoculations of local cultivar of *C. procera* seedlings led to leaf lesion development, confirming the pathogenicity of *N. cynanchi* on *C. procera*. None of the reported fungal species on *C. procera* in Iran, including *P. calotropidis A. calotropidis*, and *Alternaria* sp. (Ershad 2022); have been identified during our surveys on this plant. It is not evident whether these fungi are pathogenic on *C. procera*, since there is a lack of detailed information regarding their morphology, biology and phylogeny in existing studies. This disease can have significant economic and social impacts, given that *C. procera* is widely used in Persian traditional medicine. Our field observations indicated that *N. cynanchi* has caused considerable damage to *C. procera* shrubs in regions where the pathogen was detected. However, the incidence as well as economic and ecological impact of the disease, remaines to be studied. More information on the disease cycle and epidemiology is required to develop effective management recommendations.

ACKNOWLEDGMENTS

This research has been supported by the Institute of Science and High Technology and Environmental Sciences, Graduate University of Advanced Technology, Kerman, Iran, under grant number of 02/2816.

REFERENCES

Ahmad Nejhad, A., Alizadeh Behbahani, B., Hojjati, M., Vasiee, A. and Mehrnia, M. A. 2023. Identification of phytochemical, antioxidant, anticancer and antimicrobial potential of *Calotropis procera* leaf aqueous extract. Scientific Reports 13(1): 14716.

Ahmadpour, S.A., Mehrabi-Koushki, M. and Farokhinejad, R. 2017. *Neodidymelliopsis farokhinejadii*, a new fungal species from dead branches of trees in Iran. Sydowia 69: 171–182.

Al-Rowaily, S.L., Abd-ElGawad, A.M., Assaeed, A.M., Elgamal, A.M., Gendy, A.E.N.G.E. et al. 2020. Essential oil of *Calotropis procera*: Comparative chemical profiles, antimicrobial activity, and allelopathic potential on weeds. Molecules 25(21): 5203.

Aveskamp, M.M., de Gruyter, J. and Crous, P.W. 2008. Biology and recent developments in the systematics of *Phoma*, a complex genus of major quarantine significance. Fungal Diversity 31: 1–18.

Aveskamp, M.M., de Gruyter, J., Woudenberg, J.H.C., Verkley, G.J.M. and Crous P.W. 2010. Highlights of the Didymellaceae: a polyphasic approach to characterize *Phoma* and related pleosporalean genera. Studies in Mycology 65: 1–60.

Barreto, R.W., Evans, H.C. and Pomella, A.W. 1999. Fungal pathogens of *Calotropis procera* (rubber bush), with two new records from Brazil. Australasian Plant Pathology 28: 126–130.

Chen, Q., Hou, L.W., Duan, W.J., Crous, P.W. and Cai, L. 2017. Didymellaceae revisited. Studies in Mycology 87(1): 105–159.

Chen, Q., Jiang, J.R., Zhang, G.Z., Cai, L. and Crous, P.W. 2015. Resolving the *Phoma* enigma. Studies in Mycology 82: 137–217.

Choi, Y.W., Hyde, K.D. and Ho, W.H. 1999. Single spore isolation of fungi. Fungal Diversity 3: 29–38.

Crous, P.W., Verkley, G.J.M., Groenewald, J.Z. and Samson, R.A. 2009. Fungal biodiversity. CBS Laboratory Manual Series, 1. Westerdijk Fungal Biodiversity Institute, Utrecht, Netherlands.

De Gruyter, J., Aveskamp, M.M., Woudenberg, J.H.C., Verkley, G.J., Groenewald, J.Z. and

Crous, P.W. 2009. Molecular phylogeny of *Phoma* and allied anamorph genera: towards a reclassification of the *Phoma* complex. Mycological Research 113: 508–519.

Doyle, J.J. and Doyle J.L. 1987. A rapid DNA isolation procedure for small quantities of fresh leaf tissue. Phytochemical Bulletin 19:11-15.

Ershad, D. 2022. Fungi and Fungal Analogues of Iran. Iranian Research Institute of Plant Protection, Tehran, Iran.

Farrar, N., Sadeghi, S.M., Golestaneh, S.R. and Karampour, F. 2020. Values, benefits and use of *Calotropis procera* in Southern Iran. Iran Nature 5(1): 41–48.

Ghasemi, S., Ghasemi, M., Moradi, N. and Shamili, A. M. 2012. Effect of *Calotropis procera* leaf extract on seed germination of some plants. Journal of Ornamental and Horticultural Plants 2(1): 27–32

Glass, N.L. and Donaldson, G.C. 1995. Development of primer sets designed for use with the PCR to amplify conserved genes from filamentous ascomycetes. Applied and Environmental Microbiology 61(4): 1323–1330.

Hassan, L.M., Galal, T.M., Farahat, E.A. and El-Midany, M.M. 2015. The biology of *Calotropis procera* (Aiton) WT. Trees 29: 311–320.

Hou, L.W., Groenewald, J.Z., Pfenning, L.H., Yarden, O., Crous, P.W. and Cai, L. 2020. The *phoma*-like dilemma. Studies in Mycology 96: 309–396.

Liu, Y.J., Whelen, S. and Hall, B.D. 1999. Phylogenetic relationships among ascomycetes: evidence from an RNA polymerase II subunit. Molecular Biology and Evolution 16: 1799–1808.

Peever, T.L., Canihos, Y., Olsen, L., Ibanez, A., Liu, Y-C. and Timmer, L.W. 1999. Population genetic structure and host specificity of *Alternaria* spp. causing brown spot of *Minneola tangelo* and rough lemon in Florida. Phytopathology 89: 851–860.

Posada, D. 2008. jModelTest: phylogenetic model averaging. Molecular biology and evolution *25*(7): 1253–1256.

Qian, Z., Zhang, S., Manawasinghe, I.S., Sun, D., Song, J. and Xu, B. 2024. Taxonomic revision of *Neodidymelliopsis* with *N. cynanchi* sp. nov., associated with *Cynanchum sibiricum* leaf spot in Xinjiang, China. New Zealand Journal of Botany 62(2-3): 151–164.

Rahman, M.A. and Wilcock, C.C. 1991. A taxonomic revision of *Calotropis* (Asclepiadaceae). Nordic Journal of Botany 11: 301–308.

Rambaut, A. 2012. FigTree Version 1.4.0. Available online: http:// tree.bio.ed.ac.uk/software/figtree/ (accessed on 20 February 2024).

Razaghi, P. and Zafari, D. 2018. Characterization of fungi causing lesion blight on *Papaver dubium* in Iran. Antonie Leeuwenhoek 111: 437–455.

Rehner, S.A. and Samuels, G.J. 1994. Taxonomy and phylogeny of *Gliocladium* analysed from nuclear large subunit ribosomal DNA sequences. Mycological Research 98: 625–634.

Ronquist, F., Teslenko, M., Van Der Mark, P., Ayres, D.L., Darling, A., et al. 2012. MrBayes 3.2: efficient Bayesian phylogenetic inference and model choice across a large model space. Systematic Biology 61: 539–542.

Soleimani, P., Soleimani, M.J. and Hosseini, S. 2018. Phylogenetic relationship and evolution of *Neodidymelliopsis* isolates collected from Iran. Mycosphere 9(6): 1235–1255.

Sung, G.H., Sung, J.M., Hywel-Jones, N.L. and Spatafora, J. 2007. A multi-gene phylogeny of Clavicipitaceae (Ascomycota, Fungi): identification of localized incongruence using a combinational bootstrap approach. Molecular Phylogenetics and Evolution 44: 1204–1223.

Thompson, J.D., Gibson, T. and Higgins, D.G. 2002. Multiple sequence alignment using ClustalW and ClustalX. Current protocols in bioinformatics 2.3.1–2.3. 22.

Vilgalys, R. and Hester, M. 1990. Rapid genetic identification and mapping of enzymatically amplified ribosomal DNA from several *Cryptococcus* species. Journal of Bacteriology 172: 4238–4246.

White, T.J., Bruns, T., Lee, S., and Taylor, J.W. 1990 Amplification and direct sequencing of fungal ribosomal RNA genes for phylogenetics. In: Innis PCR Protocols, A Guide to Methods and Applications (M.A. Innis, D.H. Gelfand, J.J. Sninsky & T.J. White eds): 315–322. Academic Press, New York, USA.

Wilkinson, P.M., Thomas-Hall, S., Marney, T.S. and Shivas, R.G. 2005. First record of *Passalora calotropidis* in Australia and its generic position. Australasian Plant Pathology 34: 95–98.

شناسایی و توصیف *Neodidymelliopsis cynanchi*، عامل لکه‌برگی استبرق

آزاده حبیبی[1]✉ و رضا مستوفی‌زاده قلمفرسا[2]

۱- گروه تنوع زیستی، پژوهشگاه علوم و تکنولوژی پیشرفته و علوم محیطی، دانشگاه تحصیلات تکمیلی صنعتی و فناوری پیشرفته، کرمان، ایران.

۲- بخش گیاه‌پزشکی، دانشکده کشاورزی، دانشگاه شیراز، شیراز، ایران

چکیده: استبرق (*Calotropis procera*) درختچه یا درخت کوچکی است که در مناطق گرمسیری استان‌های جنوبی ایران می‌روید. از مزایای اقتصادی این درختچه می‌توان به استفاده از شیرابه و عصاره‌ی آن در طب سنتی اشاره کرد. در بررسی انجام شده در استان های جنوبی ایران، علائم لکه‌برگی روی درختچه‌های استبرق مشاهده شد. هدف از این مطالعه شناسایی و توصیف بیمارگرهای احتمالی ایجادکننده‌ی این علائم بود. از کشت بافت‌های آلوده، عمدتاً جدایه‌هایی از یک قارچ متعلق به خانواده *Didymellaceae*از *Ascomycota* به دست آمد. بر اساس ویژگی‌های ریخت‌شناختی و واکاوی فیلوژنتیکی چندژن‌گاهی با استفاده از توالی‌های ITS، LSU، *rpb2* و*tub2*، عامل ایجاد این لکه‌برگی، *Neodidymelliopsis cynanchi* شناسایی شد. آزمایش‌های بیماری‌زایی روی نهال‌های چهار ماهه‌ی استبرق نشان داد که جدایه‌ها باعث ایجاد لکه برگی مشخص روی میزبان می‌شوند. این اولین گزارش از ایجاد بیماری ناشی از *N. cynanchi* روی *C. procera* در جهان و نخستین گزارش از وقوع این گونه در ایران است.

کلمات کلیدی: بیماری‌زایی، ریخت‌شناسی، واکاوی فیلوژنتیک، *Calotropis procera*، *Didymellaceae*.

مکاتبه کننده: آزاده حبیبی Email: a.habibi@kgut.ac.ir

تاریخ دریافت: ۲۰/۰۹/۱۴۰۳ تاریخ پذیرش: ۲۶/۰۹/۱۴۰۳